Published in final edited form as:
*Dev Biol*. 2014 March 15; 387(2): 229–239. doi:10.1016/j.ydbio.2014.01.006.

# INO80-dependent regression of ecdysone-induced transcriptional responses regulates developmental timing in *Drosophila*

**Sarah D. Neuman**[a,b,‡], **Robert J. Ihry**[a,b,‡], **Kelly M. Gruetzmacher**[a,c,1], and **Arash Bashirullah**[a,b,2]

[a]Division of Pharmaceutical Sciences, University of Wisconsin-Madison, Madison, WI 53705, USA

[b]Cellular and Molecular Biology Graduate Program, University of Wisconsin-Madison, Madison, WI 53705, USA

[c]College of Agricultural and Life Sciences, University of Wisconsin-Madison, Madison, WI 53705, USA

## Abstract

Sequential pulses of the steroid hormone ecdysone regulate the major developmental transitions in *Drosophila*, and the duration of each developmental stage is determined by the length of time between ecdysone pulses. Ecdysone regulates biological responses by directly initiating target gene transcription. In turn, these transcriptional responses are known to be self-limiting, with mechanisms in place to ensure regression of hormone-dependent transcription. However, the biological significance of these transcriptional repression mechanisms remains unclear. Here we show that the chromatin remodeling protein *ino80* facilitates transcriptional repression of ecdysone-regulated genes during prepupal development. In *ino80* mutant animals, inefficient repression of transcriptional responses to the late larval ecdysone pulse delays the onset of the subsequent prepupal ecdysone pulse, resulting in a significantly longer prepupal stage. Conversely, increased expression of *ino80* is sufficient to shorten the prepupal stage by increasing the rate of transcriptional repression. Furthermore, we demonstrate that enhancing the rate of regression of the mid-prepupal competence factor *βFTZ-F1* is sufficient to determine the timing of head eversion and thus the duration of prepupal development. Although *ino80* is conserved from yeast to humans, this study represents the first characterization of a *bona fide ino80* mutation in any metazoan, raising the possibility that the functions of *ino80* in transcriptional repression and developmental timing are evolutionary conserved.



[2]Corresponding author: Arash Bashirullah, Division of Pharmaceutical Sciences, University of Wisconsin, Madison, WI 53705-2222. bashirullah@wisc.edu. Phone: (608) 890-1851.
[‡]S.D.N. & R.J.I. contributed equally to this work
[1]present address: School of Dentistry, University of Minnesota, Minneapolis, MN 55455, USA

**Keywords**

developmental timing; chromatin remodeler; ecdysone; transcriptional repression

## Introduction

In all metazoans, the life cycle is divided into discrete stages, including embryonic development, a juvenile growth phase, sexual maturation, and reproductive adulthood. In *Drosophila*, these stages correspond to embryogenesis, three instars of larval development, metamorphosis with prepupal and pupal stages, and adulthood. The transition between each of these developmental stages is regulated by the steroid hormone 20-hydroxyecdysone (Riddiford, 1993), henceforth referred to as ecdysone. At the onset of each transition, a systemic pulse of ecdysone triggers the appropriate morphological and behavioral changes, causing the animal to progress forward in development toward adulthood. After a developmental transition has occurred, the ecdysone pulse recedes, only to be triggered again when the animal reaches the next developmental transition. Therefore, the duration of each developmental stage is determined by the timing of ecdysone pulses.

At the onset of metamorphosis, two sequential pulses of ecdysone regulate the transformation of a crawling larva into an immature adult. These two pulses outline the boundaries of prepupal development, an intermediate stage during which adult tissues undergo morphogenesis and obsolete larval tissues are destroyed (Robertson, 1936). The first pulse, referred to as the late larval pulse, triggers puparium formation, signaling the transition from larval development to prepupal development. The second pulse, referred to as the prepupal pulse, triggers head eversion, signaling the end of prepupal development and the start of pupal development. The duration of prepupal development is one of the most tightly regulated stages during the fly life cycle, with most animals in a population completing the stage within an hour of one another (Bainbridge and Bownes, 1981).

Ecdysone, like all steroid hormones, acts through its nuclear receptor to directly regulate transcription of target genes. These transcriptional responses not only initiate stage- and tissue-specific biological responses, but also play a critical role in regulating the onset of the subsequent pulse of ecdysone, particularly during prepupal development (Thummel, 1996). Following the late larval ecdysone pulse, the early gene *E74A* is directly induced by ecdysone (Burtis et al., 1990). The early-late gene *DHR3* is also regulated by ecdysone signaling, but additional factors are required for maximal expression, resulting in delayed induction compared to early genes like *E74A* (Horner et al., 1995; Huet et al., 1995). *DHR3* then induces expression of the mid-prepupal competence factor *βFTZ-F1* (Lam et al., 1999; 1997; White et al., 1997). In turn, *βFTZ-F1* expression is required to initiate the prepupal pulse of ecdysone (Broadus et al., 1999; Woodard et al., 1994), whereupon *E74A* is induced again. In this manner, the late larval pulse of ecdysone initiates a sequential wave of gene activation that determines the timing of the prepupal ecdysone pulse and the duration of prepupal development.

The sequential transcriptional responses during prepupal development are subject to elaborate mechanisms that ensure timely repression of hormone-dependent gene expression.

Many of the protein products of these ecdysone-induced genes repress their own transcription. For example, at the prepupal pulse of ecdysone, E74A protein binds the *E74A* genomic locus and inhibits ecdysone-dependent transcription, resulting in a sharp and self-limiting peak of *E74A* mRNA expression (Ihry et al., 2012; Urness and Thummel, 1990). βFTZ-F1 is thought to have a similar auto-inhibitory property (Woodard et al., 1994). In addition to auto-inhibitory regulation, ecdysone-regulated genes exhibit cross-inhibitory regulation. For example, DHR3 protein represses *E74A* mRNA transcription after the late larval ecdysone pulse (Lam et al., 1997), ensuring that *E74A* levels decrease as DHR3 levels increase. Together, these transcriptional repression mechanisms help generate the sharp peaks and proper sequence of transcription in response to ecdysone pulses. However, despite ample evidence for mechanisms regulating repression of ecdysone-induced transcription, the biological significance of these mechanisms remains unclear.

The INO80 complex is one of the most highly conserved chromatin remodelers (Clapier and Cairns, 2009). The INO80 protein contains two functional domains: an N-terminal helicase-SANT-associated/post-HSA (HSA/PTH) domain and a Snf2 ATPase domain, which is split by a spacer region into N-terminal and C-terminal regions (Watanabe and Peterson, 2010). Each of these domains is required for binding to specific proteins that together comprise the INO80 chromatin remodeling complex, the composition of which is highly conserved from yeast to humans (R. C. Conaway and J. W. Conaway, 2009). INO80, together with its protein partners, facilitates ATP-dependent nucleosome sliding (Jin et al., 2005; Shen et al., 2000). Studies in yeast reveal that *ino80* is required for proper transcriptional regulation of many target genes (Jónsson et al., 2004; Shimada et al., 2008), and *in vitro* biochemical studies in yeast reveal that *ino80* tends to relocate nucleosomes from the edges of DNA fragments toward the center (Shen et al., 2003). Recent biochemical studies in a *Drosophila* cell culture system reveal that *ino80* primarily functions by increasing nucleosome density at its target loci (Moshkin et al., 2012), likely helping to establish repressive chromatin signatures and inhibit transcription of target genes. Despite a high level of evolutionary conservation, studies of INO80 function have been largely limited to biochemical analysis, as mutant alleles have only been characterized in yeast and *Arabidopsis* (Fritsch et al., 2004; Shen et al., 2000).

Here, we report the identification and characterization of the first metazoan mutant of *ino80*. We demonstrate that *ino*80 function is essential for development, with mutant animals arresting during metamorphosis. This lethality can be rescued by ectopic expression of *ino80* from a transgenic construct. By focusing on prepupal development, we show that mutation of *ino80* results in defects in the timely repression of ecdysone-induced transcription. Importantly, the biological consequence of these repression defects is an extended duration of prepupal development. Moreover, increased expression of *ino80* reduces the duration of prepupal development, suggesting that *ino80*-dependent regression is critical for developmental timing. We also show that the rate of regression of the mid-prepupal competence factor *βFTZ-F1* is critical to determine the timing of head eversion and the duration of prepupal development. These results provide the first characterization of *ino80* function in a metazoan organism, and also provide novel insights linking transcriptional repression mechanisms with regulation of developmental timing.

## Materials And Methods

### Stocks and recombination mapping

The following stocks were obtained from the Bloomington *Drosophila* Stock Center: *Df(3R)ED5942, Df(3R)DI-BX12, Df(3R)BSC475,* P{EPgy2}*Ino80*$^{EY09251}$, Δ*2-3 transposase, tubulin-Gal4, UAS-Dcr-2, Sgs3-GFP*. *ino80* RNAi KK102202 was obtained from the Vienna *Drosophila* RNAi Center. The *ino80*$^{psg25}$ mutation was generated in an EMS mutagenesis screen (Wang et al., 2008). C. Thummel (University of Utah, Salt Lake City, UT) kindly provided the *hs-E74A* and hs-βFTZ-F1 stocks. The dominant marker recombination mapping method used to identify *ino80*$^{psg25}$ is described elsewhere (Sapiro et al., 2013). Experiments with hemizygous *ino80*$^{psg25}$ mutant animals used the *Df(3R)ED5942* chromosomal deficiency.

### Developmental staging and lethal phase analysis

Animals were raised on standard cornmeal molasses medium in the presence of yeast in an environmental chamber set to 25°C. For developmental staging during metamorphosis, animals were synchronized either at puparium formation (white prepupa) or pupation (head eversion), placed on grape agar plates, and aged for the appropriate time at 25°C. Staging prior to head eversion was based on the average duration of prepupal development (puparium formation to head eversion) of each respective genotype. Standard “blue food” technique was used to stage late third instar larvae (Andres and Thummel, 1994). Additional developmental stages prior to metamorphosis were aged at 25°C from egg lay. For heat-shock treatments, animals at the appropriate stage were placed on grape agar plates sealed with Parafilm and submerged in a 37.5°C water bath for 30 minutes. Bainbridge and Bownes staging criteria was used to assign lethal phases: P1-P3 for prepupae (PP), P4-P9 for pupae (P), P10-15 for pharate adults (PA), and eclosed adults (A) (Bainbridge and Bownes, 1981).

### Developmental timing analysis

For head eversion timing, white prepupae were placed on grape agar plates and allowed to age for an appropriate time at 25°C. Aging on agar plates allowed for proper control of humidity. Animals were then scored for completed head eversion in 15 minute intervals. For eclosion timing, adult flies of the appropriate genotype were allowed to mate for two days, then transferred to fresh vials each day for three consecutive days. To determine the timing of eclosion, the vials were examined for empty pupal casings every 12 hours until all animals eclosed.

### Generation of the *ino80* transgene

The *ino80* sequence was amplified from cDNA clone SD02886 (BDGP) with the following primers: 5′ GAAATTAATACGACTCACTATAGGGAGACCGG 3′ and 5′ CGTCGACGTTAGAATTCGGCTACAAT 3′. The resulting amplicon was digested with *EcoRI*, ligated into *pCASPER-hs*, and sequence-verified. Transgenic flies were generated via standard protocols (Genetic Services, Inc.).

### Imprecise Excision

To generate excision events within the *ino80* locus, virgin females containing the viable P{EPgy2}*Ino80*$^{EY09251}$ P-element were crossed to males with the Δ*2-3* transposase. Progeny that lost the mini-white ($w^{+mC}$) marker on the P-element were selected, indicating that an excision event occurred, and stable stocks were generated from these animals. To identify imprecise excision events, each stock was screened for lethality. Complementation tests were carried out on the lethal excisions with *Df(3R)ED5942* and *ino80*$^{psg25}$ to identify potential *ino80* alleles. Standard PCR on a genomic DNA template was used to identify the deleted region in *ino80*$^{ex64}$.

A previously published report characterizes 2 excision alleles generated from mobilization of the same P-element we used (P{EPgy2}*Ino80*$^{EY09251}$), resulting in a 3 or 4 kilobase deletion, respectively, in the vicinity of the P-element (Bhatia et al., 2010). These alleles, unlike our *ino80* alleles, have a lethal phase early in development. However, these reported excision alleles were not tested for complementation with the *ino80*-containing chromosomal deficiency. Moreover, the specific location of the deletions was not directly characterized. Given that the P-element resides within a ~10 kilobase intron, it is unclear if these excision events disrupt *ino80* coding sequences. Importantly, in our excision scheme, most (27 of 28) of the excision events recovered were generated from a single locus residing outside the *ino80*-containing chromosomal deficiency. Each of the 27 lethal excision events of this complementation group has a lethal phase early in development. Thus, our results suggest that the original stock may have a second P-element, and the majority of lethal excision events affect that currently unidentified locus.

### Quantitative PCR

qPCR was performed as previously described (Ihry et al., 2012). RNA was isolated from appropriately-staged whole animals or dissected salivary glands using the RNeasy Plus Mini Kit (Qiagen). cDNA was synthesized from 100-400 ng of total RNA using the SuperScript III First-Strand Synthesis System with oligo$(dT)_{20}$ primers (Invitrogen). qPCR was performed using LightCycler 480 SYBR Green I Master Mix (Roche) on a Roche 480 LightCycler. For each experiment, target genes of interest and the reference gene *rp49* were run simultaneously on three independently-isolated control and experimental biological samples. 3-4 serial dilutions of pooled cDNA derived from samples spanning development were used to determine the amplification efficiency of the primers in each experiment. Roche LightCycler 480 Software (Version 1.5) was used to calculate cycle threshold values and melting curves for each reaction. Relative expression and standard error were calculated using Relative Expression Software Tool (REST) (Pfaffl et al., 2002). Standard error calculated by REST reflects asymmetrical tendencies in the data. Primer sequences are listed in Table S1. Primers were designed with A plasmid Editor (ApE), GenScript Real-time PCR Primer Design tool, or QuantPrime (Arvidsson et al., 2008).

### Immunofluorescence and Image Capture

Salivary glands from appropriately-staged animals were dissected, fixed, and immunostained using standard techniques (Yin et al., 2007). Primary antibodies used were rabbit α-cleaved caspase-3 (1:200; Cell Signaling) to detect activity of the caspase *Nc* (Fan

and Bergmann, 2010) and mouse α-Lamin (1:50; Developmental Studies Hybridoma Bank) to detect breakdown of a target of caspases. Secondary antibodies used were a-rabbit Cy3 (1:200; Jackson Immuno-Research Labs) and α-mouse AlexaFluor 488 (1:200; Invitrogen). DAPI was used to counterstain DNA (1:1,000; Invitrogen). Stained tissues were mounted on slides in Vectashield (Vector Laboratories). Immunofluorescence images were captured using an Olympus FLUOVIEW FV1000 confocal microscope with FV10-ASW software. Persistent salivary gland and lethal phase images were captured using an Olympus SZX16 stereomicroscope coupled to an Olympus DP72 camera with Olympus DPX2-BSW software.

### Western Blotting

Western blots were performed using standard methods as previously described (Ihry et al., 2012). 10 whole animals at the appropriate stage were homogenized in 75 μl of hi-salt lysis buffer, and total protein concentration was calculated using the Bradford assay. Transferred membranes were blocked with 5% BSA in PBST and then incubated with properly diluted primary antibodies overnight at 4°C. Primary antibodies used were mouse α-E74A (1:2,000; a gift from C. Thummel) and rabbit α-β-actin (1:1,000; Cell Signaling Technologies). Secondary antibodies used were α-rabbit IgG alkaline phosphatase-linked antibody (1:30,000; GE Healthcare) and α-mouse IgG alkaline phosphatase-linked antibody (1:30,000; Sigma). Membranes were developed for imaging with ECF substrate (GE Healthcare) and were imaged using a Storm 840 Scanner (Amersham Bioscience) with ImageQuant TL software version 7.0 (GE Healthcare).

## Results

### Identification of the first metazoan *ino80* mutant

To gain new insights into the mechanisms regulating ecdysone signaling during development, we previously conducted an EMS-based mutagenesis screen for mutations that disrupt the ecdysone-triggered destruction of the larval salivary glands during metamorphosis (Wang et al., 2008). Here, we characterize one of the mutations identified in this screen: *psg25*. Recombination mapping with pairs of dominant markers, followed by complementation tests with chromosomal deficiencies, was used to identify the region containing the *psg25* mutation (Sapiro et al., 2013). Additional complementation tests with deficiencies mapped *psg25* to a small region containing 20 genes (Fig. S1). *psg25* complemented all available lethals within the region; however, Sanger sequencing of *psg25* revealed a point mutation disrupting a donor splice site in the chromatin remodeler, *ino80*. Sanger sequencing of *psg25* cDNA confirmed that disruption of the donor splice site after the fourth exon results in the retention of a 26 base pair intron fragment, causing a frameshift leading to a nonsense mutation (Fig. 1A). When translated, *psg25* mRNA would produce a truncated INO80 protein, with loss of the C-terminal region of the Snf2 ATPase domain (Fig. 1B).

We also generated an independent allele of *ino80* via imprecise excision. We mobilized the P{EPgy2}$Ino80^{EY09251}$ P-element, located in the 12th intron of the *ino80* locus. After mobilization of the P-element, 163 flies with excision events were identified by loss of the

mini-white marker ($w^{+mC}$) on the transposable element; of these, 28 generated a lethal mutation on the excision chromosome (Fig. S2A). Of the 28 lethal mutations, only one failed to complement the *ino80*-containing chromosomal deficiency and resulted in sterile progeny when crossed to *psg25*. This allele, designated as $ino80^{ex64}$, contains a large deletion to the right of the P-element (~20 kilobases), excising most of the Snf2 ATPase domain and leaving a short stretch of P-element sequence within the *ino80* locus (Fig. S2B). The excision event also deletes several other genes located within the introns of *ino80*. The remaining 27 lethal excisions comprise a single complementation group that has a lethal phase early in development, unlike $ino80^{ex64}$ and $ino80^{psg25}$, which arrest during metamorphosis (Fig. 2B, S2C). Additionally, the 27 early lethal mutations complement $ino80^{psg25}$, $ino80^{ex64}$, and the chromosomal deficiency that deletes the entire *ino80* locus.

To confirm the gene identification of the $ino80^{psg25}$ and $ino80^{ex64}$ alleles, we conducted a rescue experiment. We generated a transgenic construct containing *ino80* cDNA under control of the heat-shock promoter (*hs-ino80*), and placed this construct in the $ino80^{psg25}$ mutant background. $ino80^{psg25}$ hemizygous ($ino80^{psg25}/Df$) and homozygous animals exhibit semi-lethality, with about 15% of the expected flies eclosing as viable, but sterile, adults (Fig. 1C). However, ubiquitous, leaky expression of *ino80* from the *hs-ino80* construct is able to rescue both the lethality and sterility observed in $ino80^{psg25}$ hemizygous and homozygous animals. Additionally, *hs-ino80* also rescues the lethality observed in hemizygous and homozygous $ino80^{ex64}$, suggesting that the other genes disrupted by the excision event in $ino80^{ex64}$ are not essential for viability. These results, together with the identical lethal phases of homozygous and hemizygous mutant animals (Fig. 2B, S2C), suggest that $ino80^{psg25}$ and $ino80^{ex64}$ are loss-of-function alleles of *ino80*. However, because $ino80^{ex64}$ disrupts additional genes, we chose to continue our analysis of INO80 function with the EMS-induced $ino80^{psg25}$ allele.

### *ino80* is primarily required at the onset of metamorphosis

To gain insights into the function of *ino80*, we first used quantitative reverse transcription real-time PCR (qPCR) to analyze the developmental profile of *ino80* mRNA expression. RNA was isolated from whole animals spanning embryogenesis through metamorphosis, and qPCR was used to quantify *ino80* mRNA levels in each developmental stage. *ino80* mRNA is expressed at low levels throughout development; however, the highest levels are observed during metamorphosis, with a peak of expression from puparium formation to two days after puparium formation (Fig. 2A).

We next determined when $ino80^{psg25}$ mutants arrest during development. Interestingly, all hemizygous mutant animals survive to enter metamorphosis, as the predicted percentage of expected progeny (one-third) is observed on the sides of vials when compared to balancer-containing siblings (33.4%, n=692). However, only a small percentage of these animals survive to reach adulthood. Most homozygous and hemizygous $ino80^{psg25}$ mutant animals arrest during pupal or pharate adult stages (Fig. 2B), and the few that do eclose are sterile (Fig. 1C). A similar lethal phase is observed in hemizygous $ino80^{ex64}$ mutant animals and in animals ubiquitously expressing *ino80-RNAi* (Fig. S2C). Although $ino80^{psg25}$ mutant animals arrest during metamorphosis, they form normal pupae or pharate adults without

visible abnormalities, demonstrating that morphogenetic processes are not disrupted by mutation of *ino80* (Fig. 2C,D). Overall, the expression profile and mutant lethal phase suggest that *ino80* plays a critical role during metamorphosis.

## Initiation of the ecdysone-dependent death response is delayed in *ino80$^{psg25}$* mutant salivary glands

To gain insights into the role of *ino80* during metamorphosis, we first analyzed the function of this gene in the ecdysone-dependent destruction of the larval salivary glands. *ino80$^{psg25}$* mutant animals (*ino80$^{psg25}$/Df(3R)ED5942*, unless otherwise indicated) exhibit a highly penetrant persistent salivary gland (PSG) phenotype (85.2%, n=54) at 24 h after puparium formation (APF) (Fig. S3A, B). The PSG phenotype is also observed in *ino80$^{ex64}$* hemizygous animals (83.7% PSG, n=37) (Fig. S3C). Importantly, other ecdysone-dependent processes, such as Sgs3 glue protein synthesis and secretion, occur normally (Fig. S3D-H), indicating that *ino80$^{psg25}$* mutant salivary glands have the ability to respond to ecdysone signals. To understand how *ino80$^{psg25}$* disrupts salivary gland destruction, we first analyzed induction of the death activators *reaper* (*rpr*) and *hid involution defective* (*hid*), which represents a point-of-no-return during the death response (Grether et al., 1995; White et al., 1996). We dissected salivary glands from control and *ino80$^{psg25}$* mutant animals staged relative to head eversion and analyzed their gene expression profiles using qPCR. As expected, control animals exhibit strong induction of both *rpr* and *hid* by 1.5 h after head eversion (AHE)(black line, Fig. 3A). In contrast, *ino80$^{psg25}$* salivary glands do not have maximal induction of *rpr* and *hid* until 3 AHE (blue line, Fig. 3A). Consistent with the observed delay in induction of *rpr* and *hid*, *ino80$^{psg25}$* salivary glands show a delay in caspase activation. At 1.5 AHE, control salivary glands have bright staining for cleaved-caspase-3 and dim staining for nuclear lamin, a substrate of caspases (Fig. 3B). In contrast, *ino80$^{psg25}$* mutant salivary glands at the same stage do not have staining for caspase activity and have bright staining for nuclear lamin (Fig. 3C). However, at 3 AHE, *ino80$^{psg25}$* mutant salivary glands exhibit caspase activity similar to that seen in control glands at 1.5 AHE (Fig. 3D). Overall, these results suggest that *ino80$^{psg25}$* delays, rather than disrupts, the ecdysone-triggered death response.

Because the death response in salivary glands is triggered by the prepupal pulse of ecdysone (Jiang et al., 1997; 2000), we next used qPCR to measure expression of ecdysone response genes in *ino80$^{psg25}$* mutant salivary glands. The prepupal ecdysone pulse occurs two hours prior to head eversion, and, as expected, control glands exhibit strong induction of *E74A*, an early gene that is directly induced by ecdysone, at this timepoint (black line, Fig. 3A). However, at the same stage in *ino80$^{psg25}$* mutant salivary glands, *E74A* has yet to be induced (blue line, Fig. 3A), suggesting a delayed onset of the prepupal ecdysone pulse. Consistent with these results, expression of *E74B*, which is repressed by high ecdysone titers, shows a corresponding delayed repression in *ino80$^{psg25}$* mutant salivary glands (Fig. 3A). Taken together, these results suggest that the timing of the prepupal ecdysone pulse is likely delayed in *ino80$^{psg25}$* mutant animals.

## Regression of transcriptional responses is delayed during *ino80*$^{psg25}$ prepupal development

To determine why the prepupal pulse of ecdysone is delayed in *ino80*$^{psg25}$ mutant animals, we analyzed the sequence of expression of ecdysone-regulated genes during prepupal development. We collected control and *ino80*$^{psg25}$ mutant whole animals staged relative to puparium formation and analyzed the expression profiles of ecdysone-regulated genes using qPCR. The samples collected span two pulses of ecdysone: the late larval pulse, which triggers puparium formation, and the prepupal pulse, which triggers head eversion and pupation. In *ino80*$^{psg25}$ mutant animals, induction of ecdysone-target genes in response to the late larval pulse occurs normally (Fig. 4A). The early gene *E74A* is induced to maximal levels at -4 APF, followed by induction of the early-late gene *DHR3*, which peaks at 2 APF. *βFTZ-F1* also reaches maximal expression levels on time, with a transcriptional peak at 8 APF. All of these genes are induced at the proper time, intensity, and sequence following the late larval pulse of ecdysone in *ino80*$^{psg25}$ mutant animals, indicating that induction of target genes is unaffected by mutation of *ino80*.

In contrast, regression of these ecdysone-regulated genes does not occur in a timely manner following the late larval pulse of ecdysone in *ino80*$^{psg25}$ mutant animals (Fig. 4A). In control animals, *E74A* transcription is shut off by 4 APF, while *E74A* expression is maintained until 6 APF in *ino80*$^{psg25}$ mutant animals. Similarly, *DHR3* and *βFTZ-F1* expression persists about two hours longer in *ino80*$^{psg25}$ compared to controls. Therefore, transcriptional responses to the late larval pulse of ecdysone are induced on time but regress two hours late in *ino80*$^{psg25}$ mutant animals. These regression defects appear to affect only a subset of genes during prepupal development. For example, the ecdysone biosynthetic genes *phantom* (*phm*), *spookier* (*spok*), *shadow* (*sad*), and *disembodied* (*dib*) are properly induced prior to the late larval pulse of ecdysone, and are properly repressed at the end of the pulse in *ino80*$^{psg25}$, although *sad* exhibits a subtle delay in repression (Fig. 4A, S4A). Additionally, *Cyp18a1*, a cytochrome P450 responsible for degradation of ecdysone, is also properly induced and repressed in *ino80*$^{psg25}$ mutant animals (Fig. 4A).

In addition, *ino80*$^{psg25}$ mutant animals also exhibit a delay in the onset of the responses to the prepupal ecdysone pulse. *E74A* expression is induced at high ecdysone titers and reflects the peak of the prepupal ecdysone pulse. In control animals, *E74A* is maximally induced by the prepupal ecdysone pulse at 10 APF, while *E74A* is not induced until 12 APF in *ino80*$^{psg25}$ mutant animals (Fig. 4A), two hours later than controls. Additionally, *E74B*, which is induced at low ecdysone titers and repressed at high ecdysone titers, shows a normal expression profile in *ino80*$^{psg25}$ mutant animals after the late larval pulse of ecdysone, but exhibits delayed induction during prepupal development (Fig. 4A), suggesting that *ino80*$^{psg25}$ does not affect the titer of the prepupal ecdysone pulse, only when it is induced. Our data thus far suggests that delayed repression of ecdysone-induced transcription after the late larval ecdysone pulse results in delayed onset of the prepupal ecdysone pulse.

### Auto-inhibition of ecdysone-induced genes is inefficient in *ino80$^{psg25}$* mutant animals

To understand the nature of the regression defects, we examined the efficiency of auto-inhibitory mechanisms in *ino80$^{psg25}$* mutant animals. Although the hyper-induction and prolonged expression of *E74A* mRNA observed in *ino80$^{psg25}$* is also observed in mutants that disrupt E74A protein translation (Ihry et al., 2012), western blots with an E74A antibody show that both control and *ino80$^{psg25}$* mutant animals have robust expression of E74A protein (Fig. S4B). We then tested the possibility that *ino80* is required to facilitate the auto-inhibitory activity of E74A protein. Precocious expression of E74A protein from a heterologous transgenic construct (*hs-E74A*) results in strong repression of the hormone-dependent transcription of endogenous *E74A* after the prepupal ecdysone pulse (Fig. 4B,C). In contrast, precocious expression of E74A protein in *ino80$^{psg25}$* mutant animals results in incomplete repression of ecdysone-dependent transcription of *E74A*. Similarly, precocious expression of βFTZ-F1 protein results in incomplete repression of endogenous *βFTZ-F1* transcription in *ino80$^{psg25}$* mutant animals compared to control animals (Fig. 4B,C). Taken together, these results show that *ino80* is required for the efficient auto-inhibitory activity of the E74A and βFTZ-F1 proteins, suggesting that the transcriptional regression defects during prepupal development are due to defects in auto-inhibition.

### Loss of *ino80* extends the duration of prepupal development

Our data thus far indicates that regression defects during *ino80$^{psg25}$* prepupal development result in delayed induction of the prepupal ecdysone pulse. Given that the prepupal ecdysone pulse triggers head eversion, we tested if the timing of head eversion was affected in *ino80$^{psg25}$* mutant animals. Control and *ino80$^{psg25}$* mutant animals were synchronized at puparium formation, then allowed to age until head eversion. Control animals begin to head evert at about 10.75 APF, and all animals complete head eversion by 12.5 APF, with about 50% of animals head everting by 11.5 APF ($HE_{50}$~11.5 APF, n=156)(black line, Fig. 5A). Control animals exhibit little variance in the duration of prepupal development, with nearly 90% of animals completing head eversion within a one-hour interval. The synchrony of this process is evident in the steep slope of the head eversion timing curve. *ino80$^{psg25}$* mutant animals do not begin head everting until about 12.5 APF, and all animals complete head eversion by 14.25 APF ($HE_{50}$~13.25 APF, n=152)(blue line, Fig. 5A), demonstrating that *ino80$^{psg25}$* animals head evert nearly two hours later than controls. A similar head eversion delay is observed in *ino80$^{ex64}$* ($HE_{50}$~13.5 APF, n=11). Despite a significant delay in the timing of head eversion, the *ino80$^{psg25}$* timing curve still exhibits a steep upward slope, suggesting that *ino80$^{psg25}$* does not disrupt the mechanisms that execute head eversion. The two hour delay in head eversion, coupled with the two hour delay in the onset of the prepupal ecdysone pulse shown above, suggest that the prolonged prepupal stage is likely a consequence of the regression defects in *ino80$^{psg25}$* mutant animals.

### Increased levels of *ino80* shorten the duration of prepupal development through acceleration of transcriptional regression

To demonstrate a causal relationship between INO80-dependent transcriptional repression mechanisms and the duration of prepupal development, we first tested whether increased expression of *ino80* could accelerate transcriptional repression and/or developmental timing.

Strikingly, increased expression of *ino80* does both. We collected control and *hs-ino80* animals staged relative to puparium formation and used qPCR for gene expression analysis, using a one-hour sampling rate during prepupal development in order to detect smaller shifts in gene expression. Leaky expression of *ino80* from the heat-inducible transgenic construct (*hs-ino80*) results in about a 20-fold increase in *ino80* mRNA levels at 25°C. In *hs-ino80* animals, transcription of *E74A* and *DHR3* in response to the late larval pulse appears to regress normally (Fig. 5B). However, *βFTZ-F1* regresses faster in *hs-ino80* animals, with significantly lower levels at 9 APF compared to controls. This accelerated regression coincides with precocious induction of *E74A* at the prepupal ecdysone pulse, one hour earlier than in controls. These results indicate that increased expression of *ino80* is sufficient to accelerate regression of *βFTZ-F1*. I importantly, *hs-ino80* animals head evert faster than control animals. Animals overexpressing *ino80* have an $HE_{50}$ of ~10.75 APF (n=151, purple line, Fig. 5A), about 45 minutes faster than control animals. Similar results were obtained with an independent insertion of the *hs-ino80* transgene ($HE_{50}$ ~10.75 APF, n=85). These effects on developmental timing were not limited to prepupal development. Control animals begin to eclose at 9.5 days after egg deposition (AED), and over 50% eclose by 11 days AED ($E_{50}$~10.75 AED, n=624) (black box, Fig. 5C). In contrast, increased expression of *ino80* results in nearly a one day acceleration of overall development ($E_{50}$~10 AED, n=906) (purple box, Fig. 5C). Although only a few $ino80^{psg25}$ animals eclose, those that do survive to adulthood eclose about one day later than controls ($E_{50}$~11.*7*5 AED, n=19) (solid blue box, Fig. 5C), demonstrating that $ino80^{psg25}$ mutants exhibit developmental delays throughout the entire life cycle. Importantly, this delay in $ino80^{psg25}$ is fully rescued by leaky expression of *ino80* from the *hs-ino80* transgene (*hs-ino80/+; $ino80^{psg25}$/Df*, $E_{50}$~10.75 AED, n=224) (dashed blue box, Fig. 5C).

## Accelerated transcriptional repression of *βFTZ-F1* is sufficient to shorten the duration of prepupal development

To confirm a causal relationship between transcriptional repression mechanisms and the duration of prepupal development, we focused on independently modifying the rate of regression of *βFTZ-F1*. To do this, we exploited the auto-inhibition assay described earlier (Fig. 4B). When βFTZ-F1 protein is expressed from a heterologous promoter prior to initiation of endogenous *βFTZ-F1* transcription, the endogenous transcriptional response is ablated (Woodard et al., 1994). However, we show that when βFTZ-F1 protein is expressed immediately after the start of endogenous transcription, it does not block induction of *βFTZ-F1*; instead it appears to accelerate regression of *βFTZ-F1* transcription. Animals were heat-shocked at 6 APF, at the start of endogenous *βFTZ-F1* expression, then collected at one-hour intervals following the heat-shock. In this assay, the endogenous transcriptional response does occur, as *βFTZ-F1* transcript levels are equal in both control and *hs-βFTZ-F1*-treated animals at 0.5 hrs after heat-shock (AHS) (Fig. 6A). However, in *hs-βFTZ-F1*-treated animals, endogenous *βFTZ-F1* transcription regresses significantly faster, with transcription shut off by 3.5 AHS, while endogenous *βFTZ-F1* transcription is still detectable at 4.5 AHS in control animals (*cf.* solid and dashed black lines, Fig. 6A). These results demonstrate that increased expression of βFTZ-F1 protein, delivered at the proper time, is sufficient to accelerate the rate of *βFTZ-F1* transcriptional regression. Importantly, this faster regression results in a dramatically shorter prepupal stage ($HE_{50}$ ~10.75 APF,

n=101), accelerating the timing of head eversion by almost 2 hours compared to comparably-treated controls (*cf.* solid and dashed black lines, Fig. 6B).

Given that auto-inhibition of *βFTZ-F1* appears to be inefficient in *ino80*$^{psg25}$ (Fig. 4C), we next analyzed the effects of ectopic βFTZ-F1 expression in the *ino80*$^{psg25}$ mutant background. Endogenous *βFTZ-F1* expression starts about one hour later in *ino80*$^{psg25}$ mutant animals compared to controls (Fig. S5A); therefore, as expected, heat-shock-induced expression of βFTZ-F1 at 6 APF abolishes the endogenous *βFTZ-F1* transcriptional response (blue dashed line, Fig. S5B) and results in prepupal lethality. These effects of precocious expression of βFTZ-F1 on survival are consistent with similar experiments in control animals (Yamada et al., 2000). However, *hs-βFTZ-F1* treatment in *ino80*$^{psg25}$ mutant animals at 7 APF, when *βFTZ-F1* transcripts are at a comparable level to controls at 6 APF (Fig. S5A), allows the endogenous *βFTZ-F1* transcriptional response to occur (Fig. 6A). Addition of βFTZ-F1 protein accelerates regression of endogenous *βFTZ-F1* in *ino80*$^{psg25}$ mutant animals (blue dashed line, Fig. 6A). Strikingly, this regression occurs slightly faster than in control animals lacking the *hs-βFTZ-F1* transgene (*cf.* blue dashed and black solid lines, Fig. 6A). As a result, head eversion in these *hs-βFTZ-F1*-treated *ino80*$^{psg25}$ mutant animals occurs nearly two hours faster ($HE_{50}$~12.25 APF, n=99) than comparably treated *ino80*$^{psg25}$ animals lacking the transgene ($HE_{50}$~14.25 APF, n=97) (*cf.* blue dashed and blue solid lines, Fig. 6B), effectively rescuing the timing of head eversion to that of control animals. Taken together, these results demonstrate that *ino80*-dependent repression of transcriptional responses, particularly those of *βFTZ-F1*, determines the duration of prepupal development.

## Discussion

The duration of the *Drosophila* life cycle is determined by the timing of ecdysone pulses that regulate each developmental transition. Here, we demonstrate the importance of regression of ecdysone-induced transcriptional responses in the regulation of developmental timing. The chromatin remodeling protein *ino80* is required for efficient repression of ecdysone-induced genes. *ino80*$^{psg25}$ mutant animals fail to shut off ecdysone-induced transcription in a timely manner, resulting in delayed onset of head eversion and prolonged prepupal development. Furthermore, accelerating regression of the mid-prepupal competence factor *βFTZ-F1* through overexpression of *ino80* or enhancement of the auto-inhibitory activity of βFTZ-F1 protein is sufficient to accelerate the timing of head eversion and shorten the duration of prepupal development. Therefore, INO80 function is required for timely regression of target genes, revealing a critical role for transcriptional regression in the timing of prepupal development.

The role of *ino80* in efficient repression of ecdysone-regulated transcriptional responses is consistent with the previously-described biochemical functions of this chromatin remodeler. Although loss of INO80 changes expression levels of a significant fraction of the yeast genome (Jónsson et al., 2004; Shimada et al., 2008), the function of INO80 in transcription appears to be primarily in modulating the kinetics of gene expression (Barbaric et al., 2007). These effects on transcription are mediated by the ability of the INO80 complex to promote ATP-dependent nucleosome sliding (Shen et al., 2000). This sliding activity results in

nucleosome eviction at some sites while increasing nucleosome density at others (Morrison and Shen, 2009), raising the question of whether the primary role of INO80 in transcription is in activation or repression of its target genes. Our data suggests that *ino80* plays a more critical role in repression of target genes in *Drosophila*. Consistent with our data, studies in a *Drosophila* cell culture system indicate that INO80 tends to increase nucleosome density at target loci (Moshkin et al., 2012).

All of the genes that show *ino80*-dependent regression defects--*E74A, DHR3*, and *βFTZ-F1*--were originally identified as ecdysone-induced "puffs" on *Drosophila* polytene chromosomes (Ashburner et al., 1974). In other words, the expression of these genes occurs on such a large scale that they elicit visible "puffs" of open chromatin on the polytene chromosomes of the larval salivary glands. Given that INO80 also appears to regulate repair and resolution of complex DNA rearrangements (R. C. Conaway and J. W. Conaway, 2009; Morrison and Shen, 2009), it is possible that INO80 is required to restore normal chromatin structure to chromosomal puffs following ecdysone-induced transcription, thereby facilitating regression of these hormone-dependent responses. Genomic studies show that INO80 binds many, but not all, loci in the genome (Moshkin et al., 2012); however, it is unclear whether there is a direct correlation between INO80 binding and target gene expression levels. Moreover, given that INO80 does not directly bind DNA *in vivo*, how INO80 selects its target genes remains unclear. One possibility is that Ying-Yang 1 (YY1), or Pleiohomeotic (Pho) in *Drosophila*, a zinc finger transcription factor that is part of the INO80 complex in all metazoans (Cai et al., 2005; Jin et al., 2005; Klymenko et al., 2006), may play that role. In fact, in human cells, YY1 plays a role in localizing the INO80 complex to some target genes (Cai et al., 2007), raising the possibility that this transcription factor aids in recognition of INO80-target genes in *Drosophila*.

Our results indicate that *βFTZ-F1* is a biologically-relevant target of *ino80*-dependent transcriptional repression. Under all experimental conditions tested, head eversion does not begin until *βFTZ-F1* transcription is shut off, showing a direct correlation between the rate of regression of *βFTZ-F1* and the onset of head eversion. Additionally, the timing of shut-off of *βFTZ-F1* directly correlates with the onset of *E74A*, raising the possibility that regression of *βFTZ-F1* serves as a temporal checkpoint for initiation of the prepupal ecdysone pulse. The mechanism by which *βFTZ-F1* regulates the prepupal ecdysone pulse has yet to be determined, although ectopic expression of βFTZ-F1 protein is sufficient to amplify early-gene expression in response to ecdysone (Woodard et al., 1994). Given that *βFTZ-F1* expression is critical at various stages of development, it is possible that the developmental delays observed in *ino80* mutant animals are mediated by its effects on repression of genes, like *βFTZ-F1*, that play a critical role in temporal checkpoints during development.

Our *ino80* data highlights a novel class of developmental timing phenotypes. Many developmental timing phenotypes disrupt the order of developmental programs. For example, heterochronic genes in *C. elegans* specify temporal cell fate decisions during development, thereby regulating the proper sequence of developmental events (Ambros, 2000; Thummel, 2001). Another class of timing phenotypes affects the ability to progress from one developmental program to the next. For example, an inability to remove ecdysone

during prepupal development prevents the transition to pupal development (Rewitz et al., 2010). Our *ino80* mutations highlight the subtle but essential role of the timely progression through development. Although the progression and order of developmental programs do not appear to be disrupted in *ino80* mutant animals, most animals fail to complete development, highlighting the importance of proper control of the timing of events during development.

## Supplementary Material

Refer to Web version on PubMed Central for supplementary material.

## Acknowledgments

We would like to thank the Bloomington *Drosophila* Stock Center, the Vienna *Drosophila* RNAi Center, and C. Thummel for fly stocks; the Developmental Studies Hybridoma Bank and C. Thummel for antibodies; the Berkeley *Drosophila* Genome Project for reagents and Genetic Services, Inc. for transgenic generation; Yunsik Kang and Nick Wleklinski for technical assistance. This work was supported by an NSF Graduate Research Fellowship Program grant (DGE-1256259) to S.D.N. and an NIH/NIGMS grant (R01 GM095944) to A.B..

## References

Ambros V. Control of developmental timing in Caenorhabditis elegans. Current Opinion in Genetics & Development. 2000; 10:428–433. [PubMed: 10889059]

Andres AJ, Thummel CS. Methods for quantitative analysis of transcription in larvae and prepupae. Methods Cell Biol. 1994; 44:565–573. [PubMed: 7535884]

Arvidsson S, Kwasniewski M, Riaño-Pachón DM, Mueller-Roeber B. QuantPrime--a flexible tool for reliable high-throughput primer design for quantitative PCR. BMC Bioinformatics. 2008; 9:465. [PubMed: 18976492]

Ashburner M, Chihara C, Meltzer P, Richards G. Temporal control of puffing activity in polytene chromosomes. Cold Spring Harb. Symp Quant Biol. 1974; 38:655–662.

Bainbridge SP, Bownes M. Staging the metamorphosis of Drosophila melanogaster. Journal of embryology and experimental morphology. 1981; 66:57–80. [PubMed: 6802923]

Barbaric S, Luckenbach T, Schmid A, Blaschke D, Hörz W, Korber P. Redundancy of chromatin remodeling pathways for the induction of the yeast PHO5 promoter in vivo. J Biol Chem. 2007; 282:27610–27621. [PubMed: 17631505]

Bhatia S, Pawar H, Dasari V, Mishra RK, Chandrashekaran S, Brahmachari V. Chromatin remodeling protein INO80 has a role in regulation of homeotic gene expression in Drosophila. Genes to Cells. 2010

Broadus J, McCabe JR, Endrizzi B, Thummel CS, Woodard CT. The Drosophila beta FTZ-F1 orphan nuclear receptor provides competence for stage-specific responses to the steroid hormone ecdysone. Molecular Cell. 1999; 3:143–149. [PubMed: 10078197]

Burtis KC, Thummel CS, Jones CW, Karim FD, Hogness DS. The Drosophila 74EF early puff contains E74, a complex ecdysone-inducible gene that encodes two ets-related proteins. Cell. 1990; 61:85–99. [PubMed: 2107982]

Cai Y, Jin J, Florens L, Swanson SK, Kusch T, Li B, Workman JL, Washburn MP, Conaway RC, Conaway JW. The mammalian YL1 protein is a shared subunit of the TRRAP/TIP60 histone acetyltransferase and SRCAP complexes. J Biol Chem. 2005; 280:13665–13670. [PubMed: 15647280]

Cai Y, Jin J, Yao T, Gottschalk AJ, Swanson SK, Wu S, Shi Y, Washburn MP, Florens L, Conaway RC, Conaway JW. YY1 functions with INO80 to activate transcription. Nature Structural & Molecular Biology. 2007; 14:872–874.

Caldwell PE, Walkiewicz M, Stern M. Ras activity in the Drosophila prothoracic gland regulates body size and developmental rate via ecdysone release. Curr Biol. 2005; 15:1785–1795. [PubMed: 16182526]

Chiang PW, Kurnit DM. Study of dosage compensation in Drosophila. Genetics. 2003; 165:1167–1181. [PubMed: 14668373]

Clapier CR, Cairns BR. The biology of chromatin remodeling complexes. Annu Rev Biochem. 2009; 78:273–304. [PubMed: 19355820]

Conaway RC, Conaway JW. The INO80 chromatin remodeling complex in transcription, replication and repair. Trends Biochem Sci. 2009; 34:71–77. [PubMed: 19062292]

Deng H, Kerppola TK. Regulation of Drosophila metamorphosis by xenobiotic response regulators. PLoS Genet. 2013; 9:e1003263. [PubMed: 23408904]

Denton D, Shravage B, Simin R, Mills K, Berry DL, Baehrecke EH, Kumar S. Autophagy, not apoptosis, is essential for midgut cell death in Drosophila. Curr Biol. 2009; 19:1741–1746. [PubMed: 19818615]

Fan Y, Bergmann A. The cleaved-Caspase-3 antibody is a marker of Caspase-9-like DRONC activity in Drosophila. Cell Death Differ. 2010; 17:534–539. [PubMed: 19960024]

Fritsch O, Benvenuto G, Bowler C, Molinier J, Hohn B. The INO80 protein controls homologous recombination in Arabidopsis thaliana. Molecular Cell. 2004; 16:479–485. [PubMed: 15525519]

Grether ME, Abrams JM, Agapite J, White K, Steller H. The head involution defective gene of Drosophila melanogaster functions in programmed cell death. Genes Dev. 1995; 9:1694–1708. [PubMed: 7622034]

Horner MA, Chen T, Thummel CS. Ecdysteroid regulation and DNA binding properties of Drosophila nuclear hormone receptor superfamily members. Dev Biol. 1995; 168:490–502. [PubMed: 7729584]

Huet F, Ruiz C, Richards G. Sequential gene activation by ecdysone in Drosophila melanogaster: the hierarchical equivalence of early and early late genes. Development. 1995; 121:1195–1204. [PubMed: 7743931]

Ihry RJ, Sapiro AL, Bashirullah A. Translational Control by the DEAD Box RNA Helicase belle Regulates Ecdysone-Triggered Transcriptional Cascades. PLoS Genet. 2012; 8:e1003085. [PubMed: 23209440]

Jiang C, Baehrecke EH, Thummel CS. Steroid regulated programmed cell death during Drosophila metamorphosis. Development. 1997; 124:4673–4683. [PubMed: 9409683]

Jiang C, Lamblin AF, Steller H, Thummel CS. A steroid-triggered transcriptional hierarchy controls salivary gland cell death during Drosophila metamorphosis. Molecular Cell. 2000; 5:445–455. [PubMed: 10882130]

Jin J, Cai Y, Yao T, Gottschalk AJ, Florens L, Swanson SK, Gutiérrez JL, Coleman MK, Workman JL, Mushegian A, Washburn MP, Conaway RC, Conaway JW. A mammalian chromatin remodeling complex with similarities to the yeast INO80 complex. J Biol Chem. 2005; 280:41207–41212. [PubMed: 16230350]

Jónsson ZO, Jha S, Wohlschlegel JA, Dutta A. Rvb1p/Rvb2p recruit Arp5p and assemble a functional Ino80 chromatin remodeling complex. Molecular Cell. 2004; 16:465–477. [PubMed: 15525518]

Klymenko T, Papp B, Fischle W, Köcher T, Schelder M, Fritsch C, Wild B, Wilm M, Müller J. A Polycomb group protein complex with sequence-specific DNA-binding and selective methyl-lysine-binding activities. Genes Dev. 2006; 20:1110–1122. [PubMed: 16618800]

Lam G, Hall BL, Bender M, Thummel CS. DHR3 is required for the prepupal-pupal transition and differentiation of adult structures during Drosophila metamorphosis. Dev Biol. 1999; 212:204–216. [PubMed: 10419696]

Lam GT, Jiang C, Thummel CS. Coordination of larval and prepupal gene expression by the DHR3 orphan receptor during Drosophila metamorphosis. Development. 1997; 124:1757–1769. [PubMed: 9165123]

Morrison A, Shen X. Chromatin remodelling beyond transcription: the INO80 and SWR1 complexes. Nat Rev Mol Cell Biol. 2009

Moshkin YM, Chalkley GE, Kan TW, Reddy BA, Ozgur Z, van Ijcken WFJ, Dekkers DHW, Demmers JA, Travers AA, Verrijzer CP. Remodelers organize cellular chromatin by counteracting

intrinsic histone-DNA sequence preferences in a class-specific manner. Mol Cell Biol. 2012; 32:675–688. [PubMed: 22124157]

Pfaffl MW, Horgan GW, Dempfle L. Relative expression software tool (REST) for group-wise comparison and statistical analysis of relative expression results in real-time PCR. Nucl Acids Res. 2002; 30:e36. [PubMed: 11972351]

Rewitz KF, Yamanaka N, O'connor MB. Steroid hormone inactivation is required during the juvenile-adult transition in Drosophila. Dev Cell. 2010; 19:895–902. [PubMed: 21145504]

Riddiford, L. Hormones and Drosophila development. In: Bate, M.; Martinez-Arias, A., editors. The Development of Drosophila Melanogaster. 1993. p. 899-939.The development of Drosophila melanogaster

Robertson CW. The metamorphosis of Drosophila melanogaster, including an accurately timed account of the principal morphological changes. Journal of morphology. 1936; 59:351–399.

Sapiro AL, Ihry RJ, Buhr DL, Konieczko KM, Ives SM, Engstrom AK, Wleklinski NP, Kopish KJ, Bashirullah A. Rapid Recombination Mapping for High-Throughput Genetic Screens in Drosophila. G3 (Bethesda). 2013; 3:2313–2319. [PubMed: 24170736]

Shen X, Mizuguchi G, Hamiche A, Wu C. A chromatin remodelling complex involved in transcription and DNA processing. Nature. 2000; 406:541–544. [PubMed: 10952318]

Shen X, Ranallo R, Choi E, Wu C. Involvement of actin-related proteins in ATP-dependent chromatin remodeling. Molecular Cell. 2003; 12:147–155. [PubMed: 12887900]

Shimada K, Oma Y, Schleker T, Kugou K, Ohta K, Harata M, Gasser SM. Ino80 chromatin remodeling complex promotes recovery of stalled replication forks. Curr Biol. 2008; 18:566–575. [PubMed: 18406137]

Thummel CS. Flies on steroids--Drosophila metamorphosis and the mechanisms of steroid hormone action. Trends Genet. 1996; 12:306–310. [PubMed: 8783940]

Thummel CS. Molecular mechanisms of developmental timing in C. elegans and Drosophila. Dev Cell. 2001; 1:453–465. [PubMed: 11703937]

Urness LD, Thummel CS. Molecular interactions within the ecdysone regulatory hierarchy: DNA binding properties of the Drosophila ecdysone-inducible E74A protein. Cell. 1990; 63:47–61. [PubMed: 2208281]

Wang L, Evans J, Andrews HK, Beckstead RB, Thummel CS, Bashirullah A. A genetic screen identifies new regulators of steroid-triggered programmed cell death in Drosophila. Genetics. 2008; 180:269–281. [PubMed: 18757938]

Watanabe S, Peterson CL. The INO80 family of chromatin-remodeling enzymes: regulators of histone variant dynamics. Cold Spring Harb. Symp Quant Biol. 2010; 75:35–42.

White K, Tahaoglu E, Steller H. Cell killing by the Drosophila gene reaper. Science. 1996; 271:805–807. [PubMed: 8628996]

White KP, Hurban P, Watanabe T, Hogness DS. Coordination of Drosophila metamorphosis by two ecdysone-induced nuclear receptors. Science. 1997; 276:114–117. [PubMed: 9082981]

Woodard CT, Baehrecke EH, Thummel CS. A molecular mechanism for the stage specificity of the Drosophila prepupal genetic response to ecdysone. Cell. 1994; 79:607–615. [PubMed: 7954827]

Yamada M, Murata T, Hirose S, Lavorgna G, Suzuki E, Ueda H. Temporally restricted expression of transcription factor betaFTZ-F1: significance for embryogenesis, molting and metamorphosis in Drosophila melanogaster. Development. 2000; 127:5083–5092. [PubMed: 11060234]

Yin VP, Thummel CS, Bashirullah A. Down-regulation of inhibitor of apoptosis levels provides competence for steroid-triggered cell death. J Cell Biol. 2007; 178:85–92. [PubMed: 17591924]

## Highlights

- We identified and characterized the first metazoan INO80 mutant
- INO80 is essential for viability, and mutant animals die during metamorphosis
- INO80 is required for efficient regression of hormone-dependent transcription
- Regression of *βFTZ-F1* is a checkpoint for the timing of head eversion
- Failure to efficiently shut-off transcription causes developmental timing defects

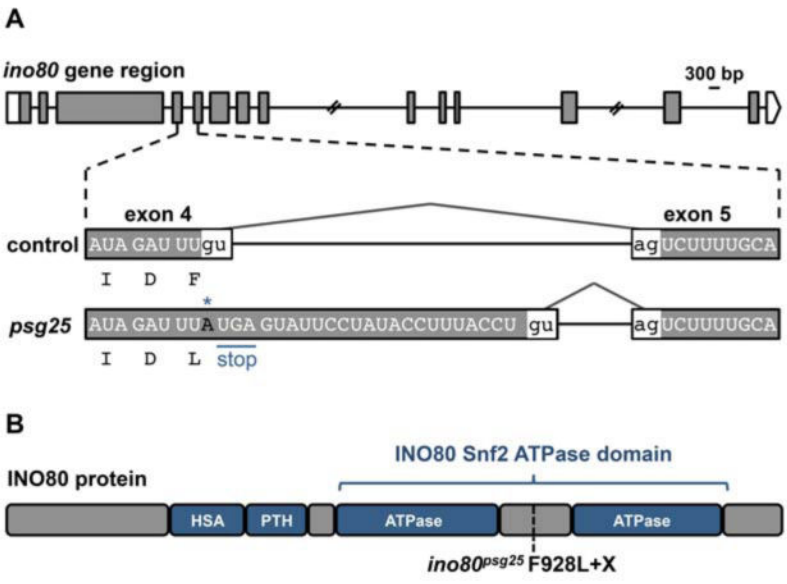


C

| genotype | *hs-ino80* | eclosed / expected (%) | sterility |
|---|---|---|---|
| *ino80$^{psg25}$/Df(3R)ED5942* | - | 14.9% (n=141) | sterile |
| | + | 84.5% (n=174) | fertile |
| *ino80$^{psg25}$/ino80$^{psg25}$* | - | 19.1% (n=173) | sterile |
| | + | 81.6% (n=114) | fertile |
| *ino80$^{ex64}$/Df(3R)ED5942* | - | 0% (n=77) | n/a |
| | + | 35.4% (n=161) | fertile |
| *ino80$^{ex64}$/ino80$^{ex64}$* | - | 0% (n=133) | n/a |
| | + | 83.5% (n=273) | fertile |

**Figure 1. Identification of a novel allele of *ino80***

**(A)** Schematic describing the *psg25* lesion in the *ino80* locus. *psg25* has a point mutation (G to A) that disrupts the donor splice site after the fourth exon, resulting in retention of an intron fragment and an in-frame stop codon immediately following the mutated donor splice site. Retention of the intron also changes a phenylalanine immediately before the donor splice site to a leucine. Boxes represent exons and shaded regions highlight coding sequences. Diagram to scale, except for two large introns, marked with slashes. Scale bar=300 base pairs (bp). **(B)** Schematic of the domains of the INO80 protein and the location of the *psg25* nonsense mutation, indicated by the dotted line. **(C)** Leaky expression of *ino80* from a *hs-ino80* transgene rescues *ino80$^{psg25}$* and *ino80$^{ex64}$*(+) or absence (−) of one copy of the *hs-ino80* transgene. Presence of the *hs-ino80* transgene also rescues the fertility of eclosing animals. Eclosion percentages expressed as observed eclosion percentage divided by expected eclosion percentage (33%).

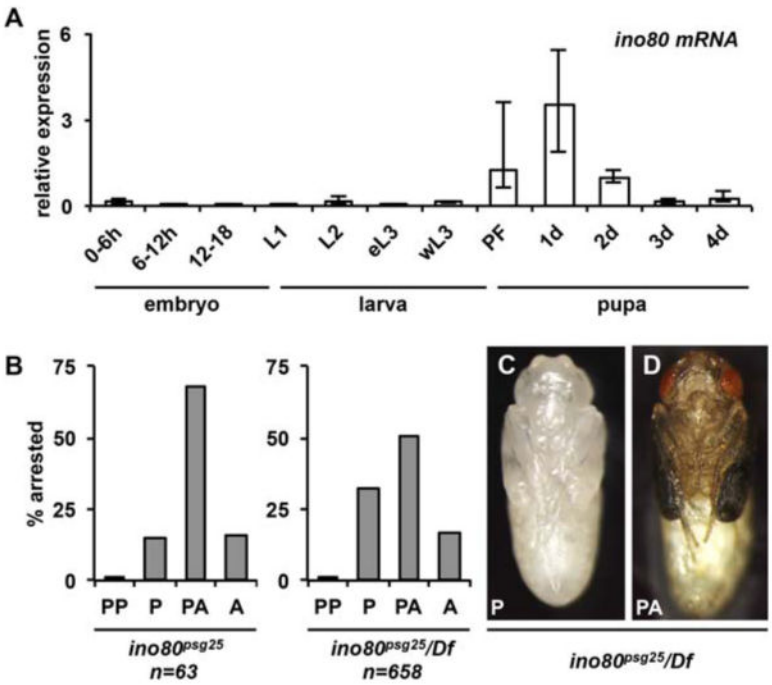


**Figure 2. *ino80*is required for viability during metamorphosis**

**(A)** qPCR analysis of *ino80* mRNA expression throughout development. The highest expression levels are observed at the onset of metamorphosis, from puparium formation to 2 days after puparium formation (APF). Animals staged from egg lay for embryonic (0-6, 6-12 and 12-18 hours after egg lay (AEL)) and larval stages (L1: 30-42 AEL, L2: 54-66 AEL, eL3: 76-88 AEL). wL3 identified by robust expression of Sgs3-GFP. Stages during metamorphosis were synchronized at puparium formation (PF) and collected in 24-hour intervals. *y*-axis plots relative expression compared to 2 days APF; *x*-axis denotes the developmental stage analyzed. Three independently-isolated whole animal samples were run for each time point and target genes were normalized to *rp49*. **(B)** Lethal phase analysis of homozygous and hemizygous $ino80^{psg25}$ mutant animals. Most homozygous and hemizygous $ino80^{psg25}$ mutant animals die after head eversion, as either pupae or pharate adults. A smaller fraction eclose as adults. **(C-D)** Hemizygous $ino80^{psg25}$ mutant animals that arrest as pupae (C) or pharate adults (D) have normal morphology, with head eversion and extension of wings and legs. Animals were dissected out of their pupal cases and imaged at their respective terminal stages. PF=puparium formation, PP=prepupa, P=pupa, PA=pharate adult, A=eclosed adult.

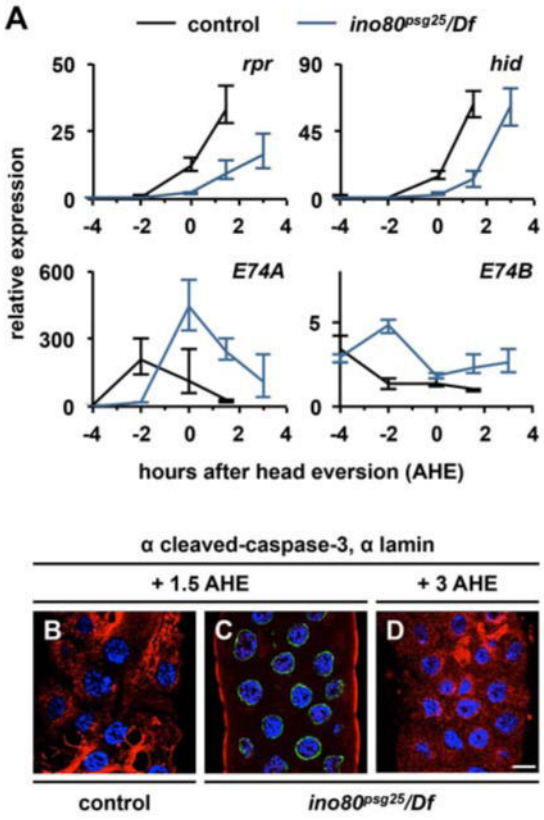


**Figure 3. Destruction of the larval salivary glands is delayed in *ino80*$^{psg25}$ mutant animals**

**(A)** qPCR analysis of target gene expression in control (black lines) and *ino80*$^{psg25}$ (blue lines) mutant salivary glands staged relative to head eversion. Control glands have strong induction of *rpr* and *hid* by 1.5 h after head eversion (AHE), while *ino80*$^{psg25}$ glands do not have maximal induction of *rpr* and *hid* until 3 AHE. Induction and regression of *E74A* and *E74B* is also delayed in *ino80*$^{psg25}$ mutant salivary glands. *y*-axis represents relative expression compared to the lowest point in control animals; *x*-axis represents developmental stage relative to head eversion. Three independently-isolated samples were run for each timepoint; relative expression calculated by normalizing to *rp49*. **(B-D)** Activation of caspases detected by staining for cleaved-caspase-3 (red) and nuclear lamin (green) in control and *ino80*$^{psg25}$ mutant salivary glands. DNA labeled with DAPI shown in blue. Control glands have ubiquitous caspase activation and strong loss of nuclear lamin staining by 1.5 AHE (B). In contrast, *ino80*$^{psg25}$ glands have caspase activation similar to controls by 3AHE (D), but not at 1.5 AHE (C). Scale bar is 20μm. AHE= after head eversion.

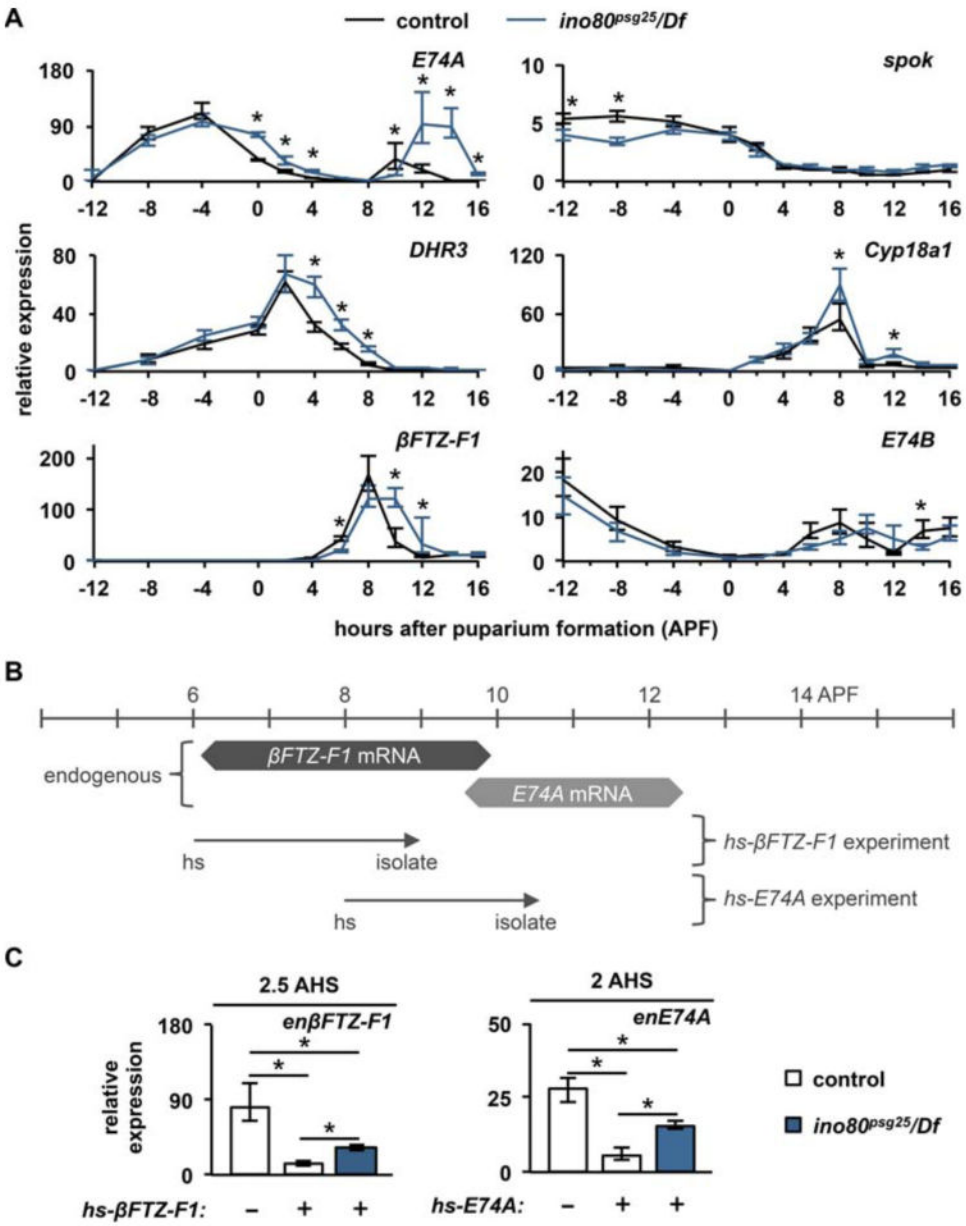


**Figure 4. *ino80 is* required for efficient regression of ecdysone-regulated genes during prepupal development**

**(A)** qPCR analysis of target genes during prepupal development in control (black lines) and *ino80*$^{psg25}$ (blue lines) mutant whole animals. The ecdysone-regulated genes *E74A, DHR3*, and *βFTZ-F1* are induced in the proper sequence in *ino80*$^{psg25}$ mutant animals following the late larval ecdysone pulse; however, *ino80*$^{psg25}$ mutant animals exhibit significant delays in repression of all three of these genes. In contrast, the ecdysone biosynthetic gene *spok*, the ecdysone turnover gene *Cyp18a1*, and the ecdysone concentration-dependent target *E74B* are unaffected in *ino80*$^{psg25}$ mutant animals. *y*-axis represents relative expression compared to the lowest point in control animals; *x*-axis represents developmental stage relative to puparium formation. Three independently-isolated whole animal samples were run for each timepoint and normalized to *rp49*. **(B)** Experimental paradigm to test efficiency of auto-inhibition by ectopic expression of the βFTZ-F1 and E74A proteins. Control and *ino80*$^{psg25}$ animals were heat-shocked two hours prior to the endogenous peak of *βFTZ-F1* (dark gray) or *E74A* (light gray) expression in each respective genotype, then allowed to recover for about 2 hours before isolation of total RNA. Timescale

shows hours after puparium formation (APF). Arrows indicate time of heat-shock and isolation. **(C)** Auto-inhibition of βFTZ-F1 and E74A occurs inefficiently in *ino80*$^{psg25}$ mutant animals. On left, expression of βFTZ-F1 protein from the *hs-βFTZ-F1* transgene is sufficient to repress endogenous *βFTZ-F1* transcription in control animals (white bars). The same treatment in *ino80*$^{psg25}$ mutant animals results in incomplete repression of endogenous *βFTZ-F1* transcription (blue bar). On right, similar results are obtained in a comparable experiment with ectopic expression of E74A. *y*-axis represents relative expression compared to the lowest point in each developmental profile; *x*-axis denotes heat-shock treatment. Asterisks denote significant differences between control and mutant samples ($p<0.05$).

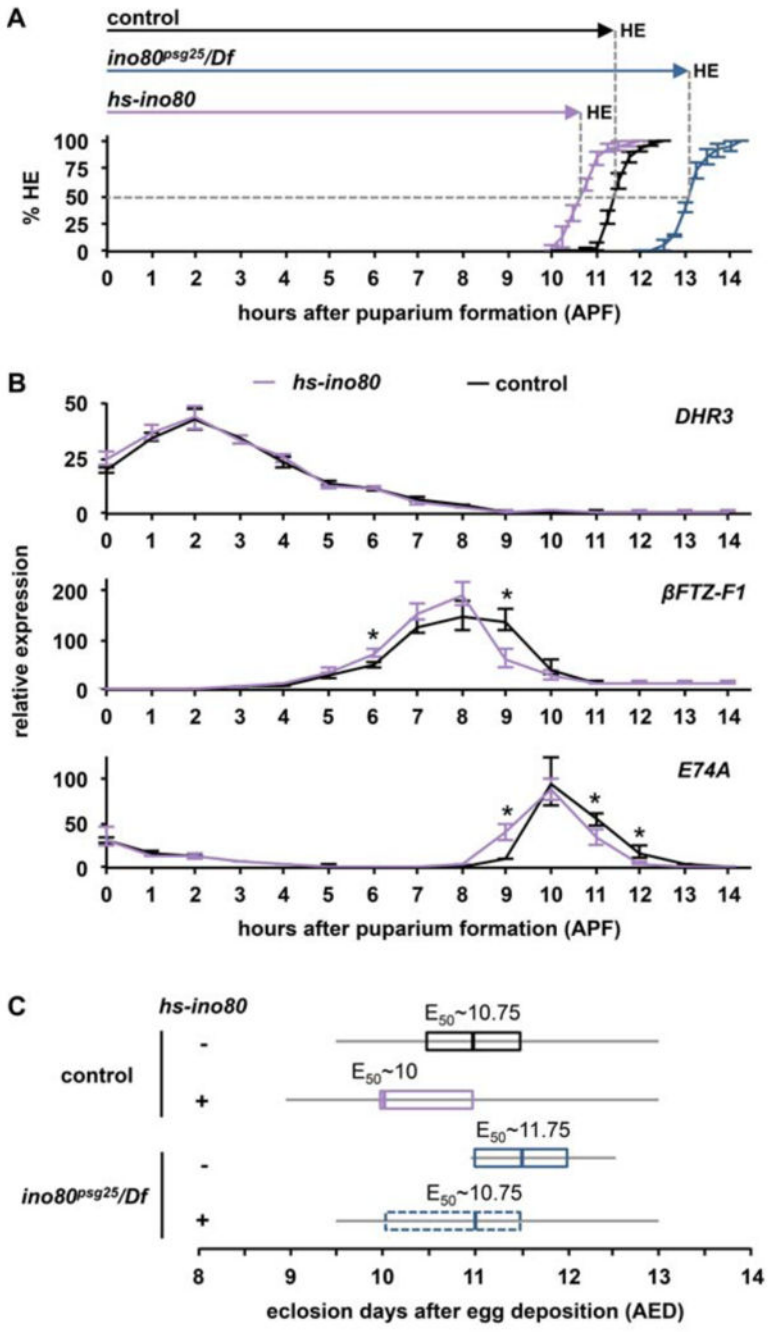


**Figure 5. *ino80* regulates the duration of development**

**(A)** Head eversion timing in control (black line), *ino80*$^{psg25}$ (blue line), and *hs-ino80* (purple line) animals. 50% of control animals head evert by 11.5 APF ($HE_{50}$~11.5, total n=156). *ino80*$^{psg25}$ mutant animals have delayed head eversion, with 50% of the animals head everting by 13.25 APF ($HE_{50}$~13.25, total n=152). *hs-ino80* accelerates head eversion, with 50% of animals head everting by 10.75 APF ($HE_{50}$~10.75, total n=151). *y*-axis plots the percentage of animals completing head eversion; *x*-axis plots time in hours relative to puparium formation (APF). Three independent samples of n~50 animals were analyzed for each genotype; error bars represent plus or minus one standard deviation. **(B)** qPCR analysis of ecdysone-regulated transcription in control (black line) and *hs-ino80* (purple line) whole animals staged relative to puparium formation. The *DHR3* expression

profile is nearly identical in control and *hs-ino80* animals. In contrast, *βFTZ-F1* regresses significantly faster in *hs-ino80* animals compared to controls. *E74A* also displays a significant acceleration in onset and repression in *hs-ino80*. *y*-axis plots relative expression compared to the lowest point in controls; *x*-axis represents stages relative to puparium formation. Three independently-isolated whole animal samples were run for each timepoint and normalized to *rp49*. Asterisks denote significant differences between control and mutant samples ($p<0.05$). **(C)** Box plot of eclosion time in control and $ino80^{psg25}$ mutant animals with or without the *hs-ino80* transgene. Control animals (black box) begin to eclose at 9.5 days AED, and 50% eclose by 10.75 AED (n=624). Few $ino80^{psg25}$ animals eclose (blue box), but those that do begin to eclose at 11 days AED, and 50% eclose by 11.75 AED (n=19). Increased expression of *ino80* from the *hs-ino80* transgene (purple box) accelerates eclosion timing, with animals beginning to eclose before 9 days AED ($E_{50}$~10 AED, n=906). Leaky expression of *ino80* from the *hs-ino80* transgene (dotted blue box) is sufficient to rescue the eclosion delay observed in $ino80^{psg25}$ mutant animals, as *hs-ino80/+;* $ino80^{psg25}$*/Df* animals begin to eclose at 9.5 days AED ($E_{50}$~10.75 AED, n=224). For each genotype, the gray horizontal lines (whiskers) represent the range for all animals analyzed, the boxes outline the middle two quartiles, and vertical lines within the boxes denote the median. *x*-axis represents time to eclosion in days after egg deposition (AED); *y*-axis shows each respective genotype plus (+) or minus (−) the *hs-ino80* transgene. The time when 50% of animals eclose ($E_{50}$) is listed for each respective genotype.

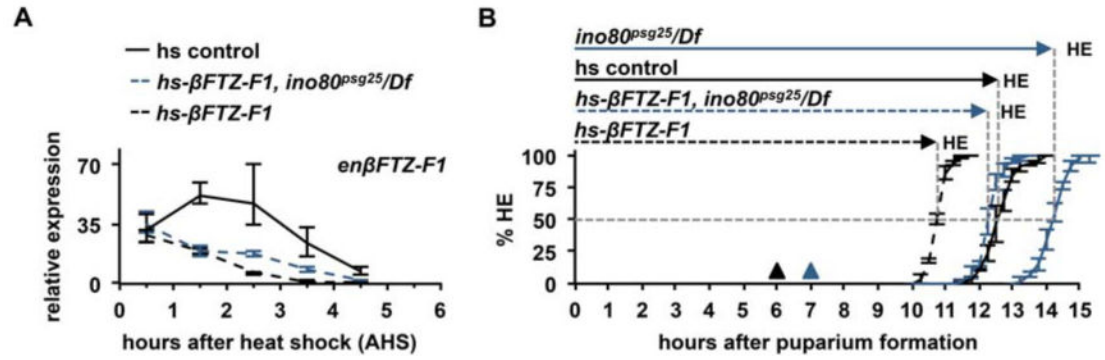


**Figure 6. Precocious transcriptional repression of endogenous *βFTZ-F1* is sufficient to accelerate developmental timing**

**(A)** Endogenous *βFTZ-F1* regresses significantly faster after expression of βFTZ-F1 protein from a heterologous promoter (*hs-βFTZ-F1*). All genotypes have similar levels of induction of endogenous *βFTZ-F1* at 0.5 hrs after heat shock (AHS). Ectopic βFTZ-F1 protein shuts off endogenous *βFTZ-F1* transcription by 3.5 AHS in control animals (dashed black line), but it takes longer in *ino80*$^{psg25}$ mutant animals (dashed blue line). *y*-axis plots relative expression compared the lowest point in the developmental profile; *x*-axis represents hours after heat-shock (AHS). Three independently-isolated whole animal samples were run for each timepoint and normalized to *rp49*. **(B)** Accelerated repression of *βFTZ-F1* is sufficient to decrease the duration of prepupal development. 50% of heat-shocked control animals head evert by 12.75 APF ($HE_{50}$~12.5 APF, total n=104). However, additional βFTZ-F1 protein accelerates the timing of head eversion by 2 hours (dashed black line, $HE_{50}$~10.75 APF, total n=101). 50% of heat-shocked *ino80*$^{psg25}$ mutants head evert by 14.25 APF (solid blue line, $HE_{50}$~14.25 APF, total n=97), but ectopic expression of βFTZ-F1 protein in the *ino80*$^{psg25}$ mutant background accelerates the timing of head eversion by about 2 hours (dashed blue line, $HE_{50}$~12.25 APF, total n=99). *x*-axis represents hours after puparium formation (APF); *y*-axis represents the percentage of animals head everted. Three independent samples of n~33 animals were analyzed for each genotype; error bars represent plus or minus one standard deviation. Triangles denote time of heat-shock in each genotype (black=control; blue=*ino80*$^{psg25}$*/Df*).